Sup fig. 1

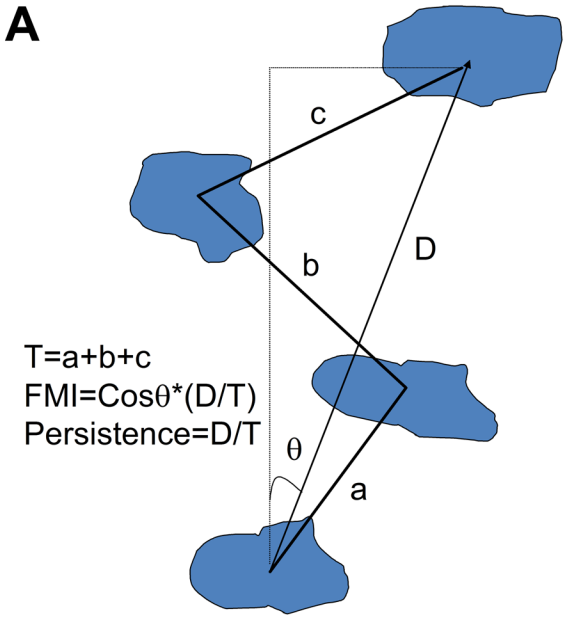
A
c
b
D
a
θ
T=a+b+c
FMI=Cosθ*(D/T)
Persistence=D/T

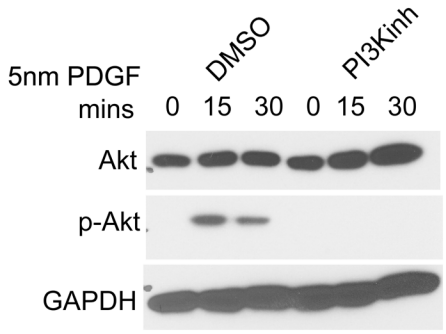
B
5nm PDGF
DMSO
PI3Kinh
mins
0 15 30 0 15 30
Akt
p-Akt
GAPDH

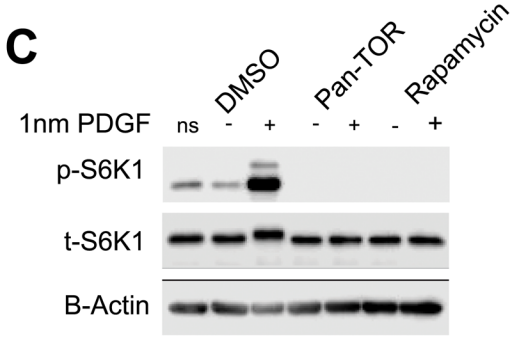
C
DMSO
Pan-TOR
Rapamycin
1nm PDGF
ns - + - + - +
p-S6K1
t-S6K1
B-Actin

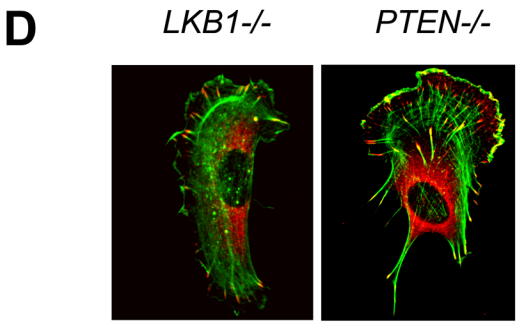
D
LKB1-/-
PTEN-/-

Sup. fig. 2

A

B *Myosin IIA KD (si2)*

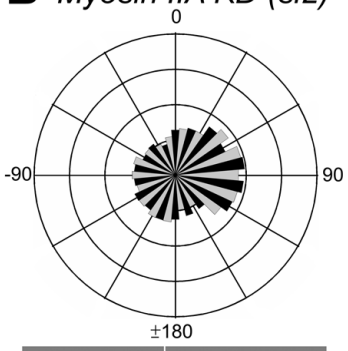

FMI	-0.03±0.05
V(μm/hr)	19.24±2.9
D/T	0.29±0.06

Myosin IIB KD (si2)

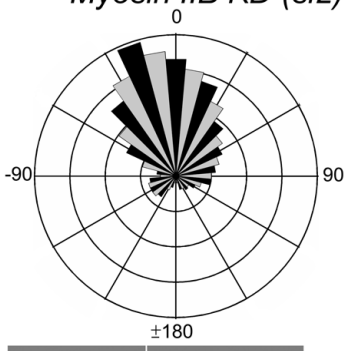

FMI	0.26±0.10
V(μm/hr)	14.45±2.40
D/T	0.48±0.06

Sup. fig. 3

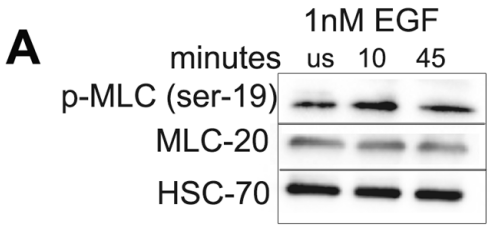
A
1nM EGF
minutes us 10 45
p-MLC (ser-19)
MLC-20
HSC-70

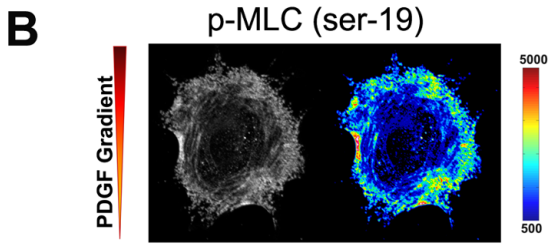
B
p-MLC (ser-19)
PDGF Gradient
5000
500

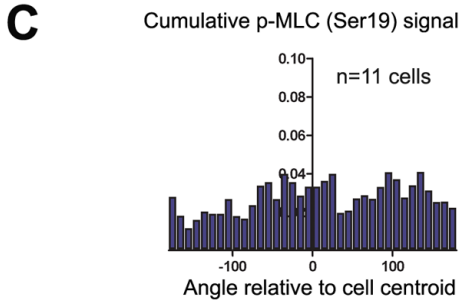
C
Cumulative p-MLC (Ser19) signal
n=11 cells
0.10
0.08
0.06
0.04
-100
0
100
Angle relative to cell centroid

Sup. fig. 4

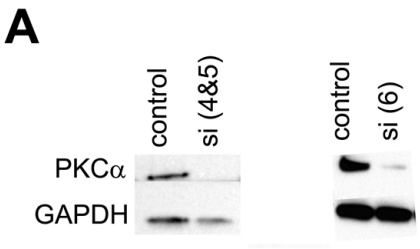

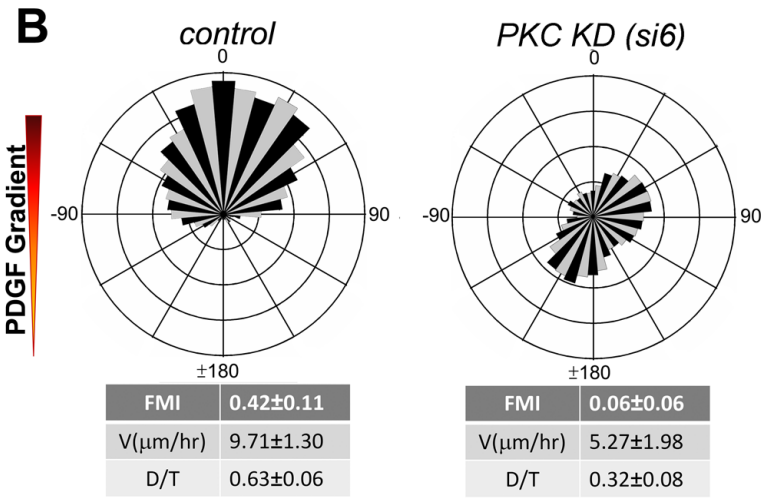

FMI	0.42±0.11
V(μm/hr)	9.71±1.30
D/T	0.63±0.06

FMI	0.06±0.06
V(μm/hr)	5.27±1.98
D/T	0.32±0.08

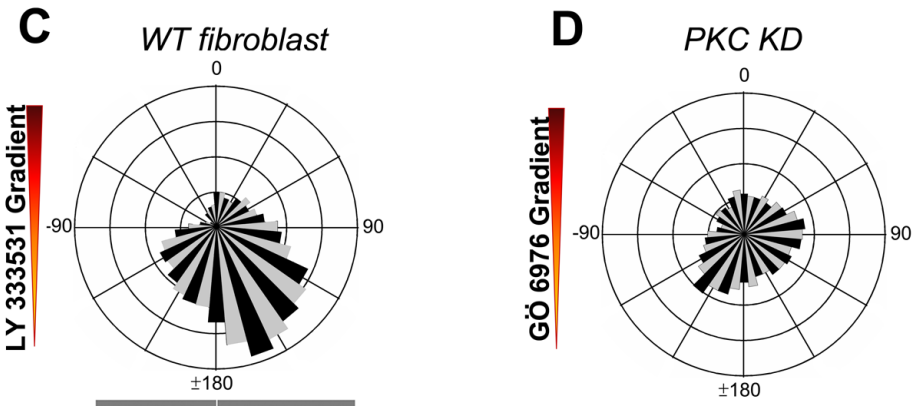

FMI	-0.20±0.08
V(μm/hr)	22.07±3.0
D/T	0.43±0.06

FMI	0.00±0.06
V(μm/hr)	25.80±1.8
D/T	0.27±0.05

Sup. fig. 5

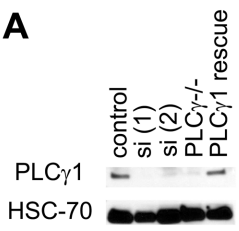

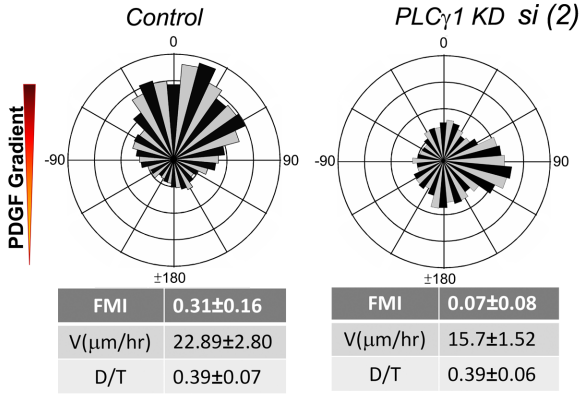

FMI	0.31±0.16
V(μm/hr)	22.89±2.80
D/T	0.39±0.07

FMI	0.07±0.08
V(μm/hr)	15.7±1.52
D/T	0.39±0.06

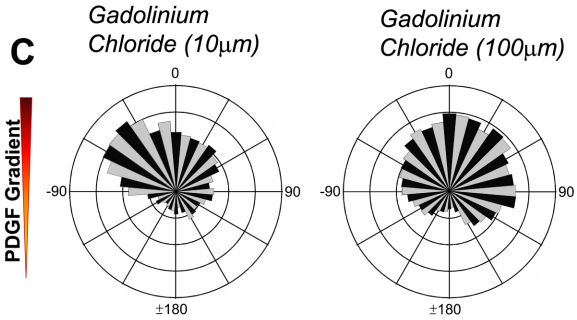

FMI	0.12±0.05
V(μm/hr)	22.57±7.2
D/T	0.30±0.06

FMI	0.13±0.06
V(μm/hr)	21.13±7.8
D/T	0.40±0.04

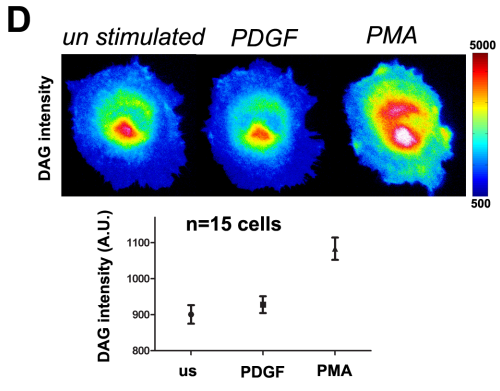

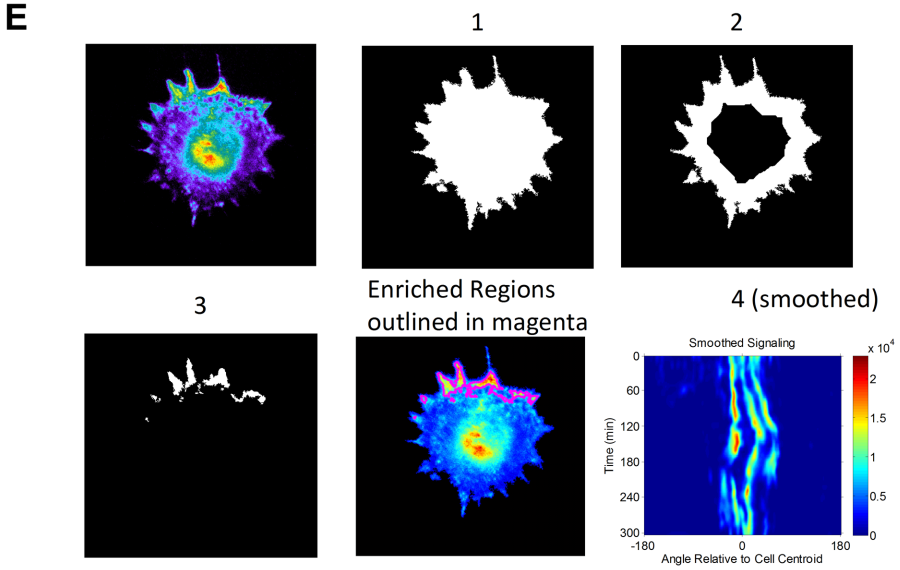

Sup. fig. 6

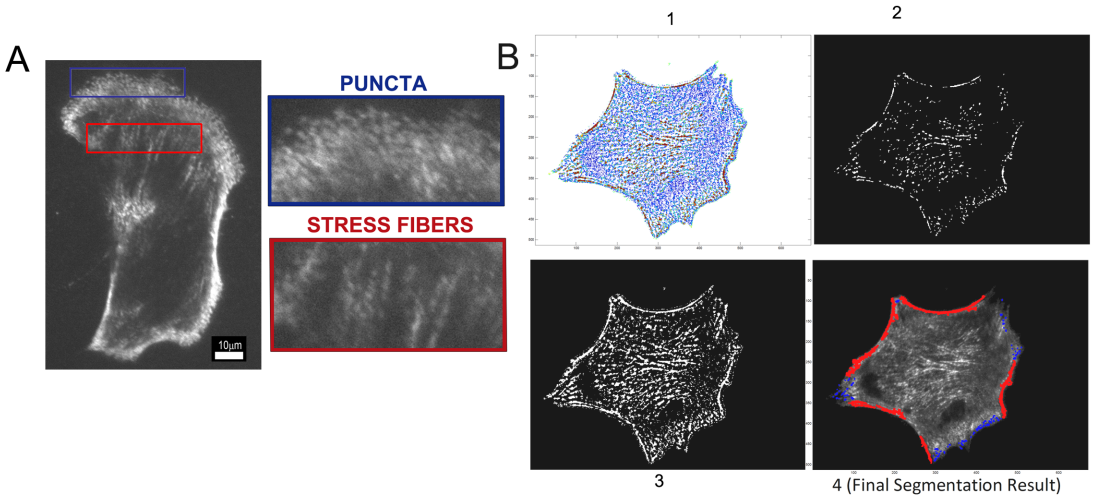
A
PUNCTA
STRESS FIBERS
10μm
B
1
2
3
4 (Final Segmentation Result)

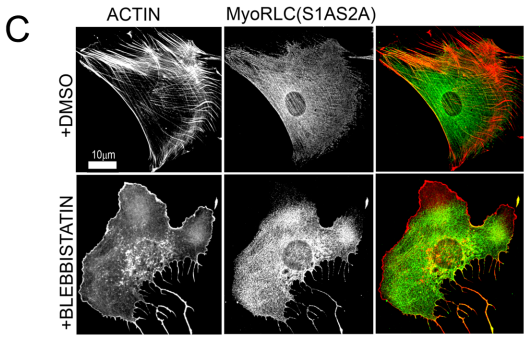
C
ACTIN
MyoRLC(S1AS2A)
+DMSO
+BLEBBISTATIN
10μm

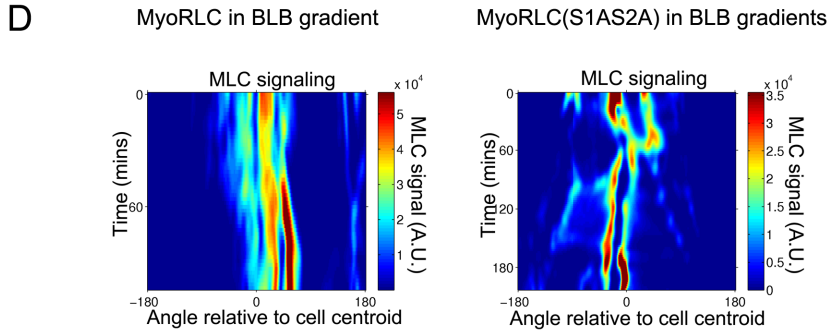
D
MyoRLC in BLB gradient
MyoRLC(S1AS2A) in BLB gradients
MLC signaling
Time (mins)
Angle relative to cell centroid
MLC signal (A.U.)
x 10^4

SUPPLEMENTAL FIGURE LEGENDS

Sup. Fig.1 (relating to main Fig. 1)

A. Schematic diagram showing FMI and persistence (D/T) calculation of a cell during chemotaxis.

B. Western blot analysis to determine phosphorylation levels of Akt in fibroblasts stimulated with PDGF for the indicated time and in the presence of PI3K inhibitor.

C. Western blot analysis to determine phosphorylation levels of S6K1 in fibroblasts stimulated with PDGF and in the presence of pan-Tor inhibitor.

D. Immunofluorescence of K-Ras/Lkb1 null (Melanoma 1) and B-Raf/Pten null (Melanoma 2) tumor cell lines shows the presence of green actin stress fibers (phalloidin) and red focal adhesions (vinculin).

Sup. Fig. 2 (relating to main Fig. 2)

A. Western blots show levels of knockdown of Myosin IIA and Myosin IIB using two different siRNAs for each myosin isoform.

B. Wind-rose plots confirm chemotactic response of Myosin IIA KD and Myosin IIB KD cells using alternate siRNAs.

Sup. Fig. 3 (relating to main Fig. 3)

A. Western blot analysis to probe the extent of Ser19 phosphorylation of Myosin II RLC, shows no change in response to EGF stimulation.

B. Example of Immunofluorescence of a chemotaxing cells stained with p-MLC (Ser-19) color coded with intensity of signal.

C. Histogram showing the cumulative intracellular distribution of p-MLC (Ser-19) in n=11 chemotaxing cells where the x-axis corresponds to the angular direction with respect to the cell centroid. Zero degrees corresponds to direction of gradient.

Sup. Fig. 4 (relating to main Fig. 4)

A. Western blots indicate levels of PKCα knockdown using multiple siRNAs.

B. Wind-rose plots confirming lack of chemotaxis of PKCα KD cells using an alternate siRNA.
C. Chemo-repulsion of wild-type cells to gradients of LY333531, an alternate conventional PKC inhibitor (n=46).
D. PKCα knockdown cells show no chemo-repulsive response to gradient of Gö6967 (n=56).

Sup. Fig. 5 (relating to main Fig. 5)
A. Western blots showing PLCγ1 content in knockdown cells, PLCγ1-/- cells and the rescue cells.
B. Wind-rose plots of directional migration of control cells and PLCγ1 KD cells with alternate siRNA.
C. Circular histograms of cells migrating in a PDGF gradient in the presence of 10μm (n=61) and 100μm Gadolinium Chloride (n=88).
D. TIRF micrographs of $(C1)_2$-GFP expressing, PLCγ1 KD cells simulated with PDGF and PMA. Graph shows average intensity of $(C1)_2$-GFP recruited to the membrane after PDGF and PMA stimulation (n=15 cells).
E. Method of analysis of the localization of DAG intensity in cells transfected with $(C1)_2$-GFP.

Sup. Fig. 6 (relating to main Fig. 7)
A. Image of a chemotaxing MLC-GFP cell. Magnified sections show myosin organization with puncta in the blue box and stress fibers in the red box.
B. A two-dimensional median filtering (1) is used to segment, puncta (2) and stress fibers (3) in the outer ring of the convex hull mask. Puncta are marked as blue and Stress fibers as red in the final segmentation (4).
C. Immunofluorescence of MyoRLC(S1AS2A) cells shows myosin light chain (GFP) and F-actin (Phalloidin) in cells before and after uniform BLB treatment.
D. The intensity values of the enriched segmented pixels in MyoRLC-GFP and MyoRLC(S1AS2A)-GFP cells chemotaxing to BLB gradient are summed within

angular bins at each time point to create a signaling “map” with the angle plotted on the horizontal axis and time on the vertical axis.

SUPPLEMENTAL MOVIE LEGENDS

Sup. Movie 1 (relating to main Fig. 1): Fibroblast cells migrating toward higher concentration of PDGF. Tracks generated during manual tracking are overlaid to show direction of migration. Images captured with 20x objective every 10 min for 6hrs.

Sup. Movie 2 (relating to main Fig. 1): Migration tracks of cells from Sup. Movie 1 are shown originating from a common center.

Sup. Movie 3 (relating to main Fig. 2): Fibroblasts in the presence of 15μm blebbistatin do not respond to PDGF gradient and migrate randomly. Gradient is marked my fluorescent dextran (red channel). Images captured 20x objective every 10 min for 12 hr.

Sup. Movie 4 (relating to main Fig. 5): Chemotaxing cell expressing GFP-tagged fragment of PKC containing tandem C1 domains as a translocation biosensor for DAG. The cell is color coded to show intensity difference in DAG localization, with high localization at the leading edge. Images were captured with a 60x TIRF objective every 2 min for 6 hr.

Sup. Movie 5 (relating to main Fig. 7): Fibroblasts expressing wild type RLC-GFP (left) and mutant S1AS2A-RLC-GFP (right) in PDGF gradients. In chemotaxing wild type cells, at the leading edge, a soluble pool of Myosin II accumulates into puncta or spots. Further away from the edge, puncta coalesce into bundled fiber-like structures consistent with localization to stress fibers. Mutants in a PDGF gradient show even distribution of puncta and stress fibers

around the perimeter of the cell. Images were captured with a 60X objective every 2 min for 6 hr.

Sup. Movie 6 (relating to main Fig. 7): Fibroblasts expressing the wild-type RLC-GFP (left) and mutant S1AS2A-RLC-GFP (right) chemotaxing to a blebbistatin gradient. At the leading edge, a soluble pool of Myosin II accumulates into puncta. Stress fibers were mostly absent in the TIRF field of view in the blebbistatin gradient. Images were captured with a 60X objective every 2 min for 6 hr.

SUPPLEMENTAL MATERIAL for

Mesenchymal chemotaxis requires selective inactivation of Myosin II at the leading edge via a non-canonical PLCγ/PKCα pathway

Asokan et al

EXTENDED EXPERIMENTAL PROCEDURES

Reagents and Materials:

AlexaFluor dyes conjugated to phalloidin were from Invitrogen. Antibodies were purchased from Cell Signaling Technology, ECM Biosciences and Santa Cruz Biotechnology. PDGF-BB was purchased from BD Biosciences and PMA from Sigma. Inhibitors of PDGF-R, PI3K and MLCK were purchased from Calbiochem, Pan-tor inhibitor, Blebbistatin and MLCK and ROCK inhibitor from Sigma Aldrich, and Gö6976 was purchased from Tocris. siRNAs were purchased as a set of four from Qiagen for Myosin IIA (GS17886), Myosin IIB (GS77579), PKCα (GS18750) and PLCγ1 (GS18803).

Cell culture, viral transduction and plasmid/siRNA transfections:

Cells were cultured in DMEM supplemented with 10% FBS (HyClone), 100 U/mL penicillin, 100 µg/ml streptomycin and 292 µg/mL L-glutamine. Transient transfections were performed using FuGene 6 (Roche) for HEK293 FT cells and NanoJuice (EMD Millipore) for fibroblast cell lines. Retroviral packaging, infections, and fluorescence-activated cell sorting were as described (Bear et al., 2000). Lentivirus production and infection were as described (Cai et al., 2008). K-Ras;LKB1-/- cells, B-Raf;Pten-/- cells and PLCγ1-/-, PLCγ1 rescue cells were kind gifts from Sharpless lab (UNC-CH), Kim lab (UNC-CH), and Sondek lab (UNC-CH). Tagged tandem C1 domains from PKCγ, $(C1)_2$-GFP, was transiently transfected into IA32 fibroblasts using NanoJuice reagent. The cells were sorted

using a Biorad S3 sorter 18 h post-transfection. The sorted cells were immediately loaded into the chemotaxis chamber for cell migration assays. siRNA for each gene was purchased as a FlexiTube Gene Solution set from Qiagen and reconstituted following manufacturer's instructions in nuclease-free water. IA32 fibroblasts were transfected at 50% confluency using 25-50pmol of siRNA and RNAiMAX transfection reagent (Life Technologies) following the manufacturer's protocol. Knockdown was analyzed by blotting and/or immunofluorescence 48-96 hours post-transfection.

Generation of Arpc2-/- fibroblasts:

Homozygous mice carrying a floxed *Arpc2* allele were maintained in an Ink4a/Arf null genetic background. All mice were maintained in IACUC approved housing and had free access to standard food and water. Euthanization of mice and harvesting of tissue was also carried out under IACUC approved protocols. Adult mice were sacrificed and tails were harvested for isolation of tissue fibroblasts. The superficial dermis was peeled away and remaining tail was minced into small pieces, which were placed directly onto gelatin-coated plates and incubated in DMEM supplemented with 10% FBS, 1% Pen/Strep, and 1% Glutamax. After five days, tail chunks were removed and bulk fibroblast cultures were expanded according to normal fibroblast culture conditions. These cells were then stably transduced with a CreER-expressing retrovirus (made with Addgene plasmid 22776) and subjected to puromycin selection. Bulk populations of puro-resistant adult tail fibroblasts were sorted as single cells into each well of a 96 well plate. Clones were continuously cultured and expanded to 10 cm dishes. Clonal lines were tested for responsiveness to tamoxifen by treatment of a subset of cells with 2 uM 4-hydroxytamoxifen (4-OHT) to stimulate CreER activity on days one and three of culture. On day five, treated (KO) cells and untreated (WT, pre-Cre) control cells were expanded and cultured side by side. At this point they were analyzed for loss of p34 (encoded by the *Arpc2* gene) via western blotting and immunofluorescence, and tested for chemotaxis. A more complete characterization of these cells will be reported separately.

Microfludic device preparation:

The pattern for the chemotaxis chamber was fabricated on 4” silicon wafers using a two-step photolithography process. The first step involved spin coating a 5 micron tall layer of SU-8 (25) from microposit and transfer of the microcapillaries to the wafer. After developing the first layer a second 100 micron tall layer of SU-8 (100) was applied to the same wafer and after alignment the channels were transferred to the wafer. After developing and post-baking, the silicon wafer was exposed to silane overnight. Polymethylsiloxane (PDMS) was poured on the wafer and cured overnight in a 70^{o} C oven. Individual PDMS devices were cut out from the wafer and placed in a clean dish until use. The sharp ends of 20 gauge needles were cut off and then smoothed using a Dremel tool. The needles were then used to punch out ports in the devices. The devices were then washed with water and ethanol, blow-dried and exposed to air plasma for 2 mins in a plasma cleaner (Harrick plasma). Glass bottom culture dishes (MatTek) or Delta T dishes (Bioptechs) dishes were cleaned using water and ethanol and then exposed to plasma for 2 mins. The PDMS device was placed in contact with glass dish immediately following plasma treatment of both pieces, ensuring that an irreversible seal was formed. The cell culture chamber was then filled with 10 µg/mL FN for 15mins at 37^{o} C, followed by flushing with sterile PBS. Cells were loaded into the cell culture chamber using a gel loading pipette tip. The cell chamber ports were plugged with short pieces of tubing (Upchurch Scientific, .0025” x 1/32”) before gradient formation.

Chemotactic gradients:

The exit ports of the sink and source channels were connected to waste using tubing of ID 0.015”. Gas tight 100 µL Hamilton glass syringes (81020,1710TLL 100ul SYR) were connected to 27 1/2 gauge needles connected to tubing. The source syringe and tubing were filled with DMEM containing indicated chemoattractant/pharmacological drug and 0.01 µg/mL of TRITC/Cy5-dextran to visualize the gradient. The sink syringe and tubing were filled with DMEM. The

tubing was then inserted into the source and sink channels respectively, and the syringe pump was operated at a flow rate of 20 nL/min. A stable gradient was then established in the cell culture chamber within 30 min, and typically remained stable for almost 24 hr as monitored by dextran fluorescence intensity.

Immunofluorescence:

For immunofluorescent staining, the cells were fixed, stained and mounted as described previously (Bear et al., 2002). Cells were plated on acid-washed coverslips coated with 10 µg/mL FN overnight before fixing with 4% PFA and permeabilized in 0.1% Triton X-100 in PBS for 5 mins. Cells were then blocked for 15 mins in PBS containing 5% normal goat serum (Jackson Laboratories) and 5% fatty-acid-free BSA. Primary antibodies were applied to cells in PBS containing 1% BSA for 1 hr at room temperature. Cells were stained in various combinations with AlexaFluor-647 phalloidin for F-actin (1:200 dilution), Myosin-RLC (MLC-20; 1:250 dilution) or Vinculin (1:250 dilution) antibodies. After washing the cells three times in PBS, fluorescent dye conjugated secondary antibodies were diluted to 1:250 in 1% BSA in PBS and applied to the coverslips for 1 hr. After three washes in PBS, the coverslips were mounted onto slides with Fluoromount G (Electron Microscopy Sciences). Images were captured using a FluoView scanning confocal inverted microscope (FV1000, Olympus) equipped with a 40x objective, a Hamamatsu PMT and controlled by Fluoview software. Maximum intensity projection was determined with ImageJ from a z-stack.

TIRF microscopy

The microfluidic chamber system is fully integrated with live-cell TIRF microscopy imaging. A 60X TIRF objective was used to image the translocation of $(C1)_2$-GFP or localization of the RLC-GFP constructs during chemotaxis. The cells were imaged at 2-minute intervals for 5-10 hours.

Analysis of the DAG pattern

A mask of the cell is created via threshholding and removing small isolated groups of pixels (Fig S5E(1)). A mask of the cell periphery is created from the whole cell mask by erosion of edges and subtracting the resulting image from the cell mask (Fig. S5E(2)). Locally enriched signaling regions are determined in the periphery mask (2) by segmenting contiguous regions (at least 15 pixels) with intensity values that exceed a set number (1.2) of standard deviations above the mean intensity of the periphery mask (Fig. S5E(3)). Any pixels completely enclosed by enriched pixels are also included (outlined in magenta). In a method similar to one described previously (Welf et al., 2012), the intensity values of the segmented pixels are summed within angular bins relative to the cell centroid in each image. This is done for each time point to create a signaling "map" (Fig. S5E(4)) with the angle plotted on the horizontal axis and time on the vertical axis. To quantify the overall signaling pattern for each cell, the values in each angular bin is averaged over all time points and then normalized such that the mean across all bins is equal to 1. These normalized patterns are then averaged over all the cells for each condition to produce an aggregate plot. The linear (unbinned) plots are smoothed by local regression using weighted linear least squares and a first-degree polynomial mode. The cumulative DAG signal is then presented as a histogram with a bin size of 10 degrees for chemotaxing cells (*n* = 12 cells) and randomly migrating (*n* = 13 cells)(Fig. 5E, 5F). A similar approach was used to analyze the distribution of pSer19 of RLC in chemotaxing cells.

Analysis of Myosin II organization

As in the analysis of DAG, masks of the cell and cell periphery are created. Due to the obscured visibility and discontinuity of the cell outline in cells expressing RLC-GFP constructs, a convex hull around the original cell mask is used to calculate the cell centroid as well as to exploit the fact that stress fibers reside almost exclusively in concave regions. Using two-dimensional median filtering (Fig. S6B(1)), puncta (Fig. S6B(2)) and stress fibers in the outer ring of the convex hull mask are segmented. A larger geometry and lower threshold is used for segmenting stress fibers due to their larger size (Fig. S6B(3)). Median-filtered

objects are organized by size, objects of only a few pixels are removed, and large objects with high aspect ratios are identified as stress fibers (any other large objects are removed). If a stress fiber is identified in one frame, median-segmented regions that overlap with it in the next frame are also considered stress fibers if they have a high aspect ratio. This aids in the detection of stress fibers that might not be fully segmented by the median filter in every frame. Each of the pixels associated with puncta is assigned to an angular bin with respect to the cell centroid (1 count per pixel); any bin containing both puncta and stress fibers are counted as stress fibers. To correct for discontinuous stress fibers missed between frames, any angular bin marked as containing stress fibers more than half the time during a 15-frame interval is marked as a stress fiber for the entire interval. After this procedure, each angular bin is classified as puncta, stress fiber, or neither. To plot the distribution of puncta, stress fiber bins are set to zero, and vice-versa for the stress fiber distribution. The plots are generated in the same manner as described above for the DAG pattern. The data for the wild-type RLC-GFP-expressing cells in the PDGF gradient are shifted by the median angle of migration (not including angles more than 90° from the direction of the PDGF gradient), resulting in a 25-degree shift to the right. During migration in response to a BLB gradient, very few stress fibers were visible under TIRF imaging. Analysis was therefore performed in the same manner as for the DAG pattern to quantify RLC-GFP regions at the cell periphery.

LITERATURE CITED

Bear, J., Loureiro, J., Libova, I., Fassler, R., Wehland, J., and Gertler, F. (2000). Negative regulation of fibroblast motility by Ena/VASP proteins. Cell *101*, 717-728.

Bear, J.E., Svitkina, T.M., Krause, M., Schafer, D.A., Loureiro, J.J., Strasser, G.A., Maly, I.V., Chaga, O.Y., Cooper, J.A., Borisy, G.G.*, et al.* (2002). Antagonism between Ena/VASP Proteins and Actin Filament Capping Regulates Fibroblast Motility. Cell *109*, 509-521.

Cai, L., Makhov, A.M., Schafer, D.A., and Bear, J.E. (2008). Coronin 1B antagonizes cortactin and remodels Arp2/3-containing actin branches in lamellipodia. Cell *134*, 828-842.
Welf, E.S., Ahmed, S., Johnson, H.E., Melvin, A.T., and Haugh, J.M. (2012). Migrating fibroblasts reorient directionality by a metastable, PI3K-dependent mechanism. J Cell Biol *197*, 105-114.